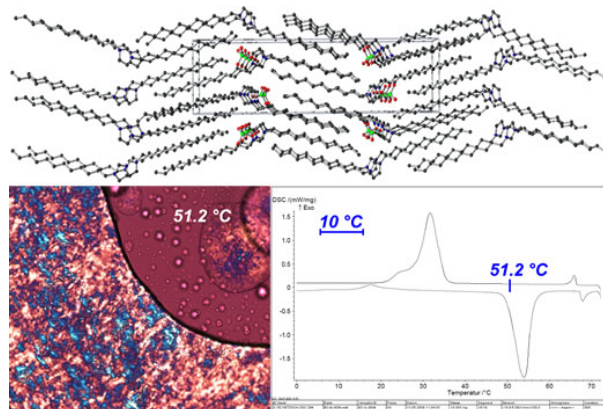


SUPPORTING INFORMATION

A new class of double alkyl-substituted, liquid crystalline imidazolium ionic liquids – a unique combination of structural features, viscosity effects, and thermal properties

Xinjiao Wang^{a)}, Frank W. Heinemann^{a)}, Mei Yang^{b)}, Berthold U. Melcher^{c)}, Melinda Fekete^{c)}, Anja-Verena Mudring^{b)}, Peter Wasserscheid^{c)*}, Karsten Meyer^{a)*}

Abstract. A new class of imidazolium based liquid-crystalline ionic liquids shows a remarkable combination of highly ordered structural features with non-Newtonian viscosity behaviour in the liquid crystalline state.



- a) Department of Chemistry and Pharmacy, Inorganic Chemistry, University Erlangen-Nuremberg, Egerlandstraße 1, D-91058 Erlangen, karsten.meyer@chemie.uni-erlangen.de
- b) Anorganische Chemie I-Festkörperchemie und Materialien, Ruhr-Universität Bochum, D-44780 Bochum, www.anjamudring.de
- c) Department of Chemical and Bioengineering, Chemical Reaction Engineering, University Erlangen-Nuremberg, Egerlandstraße 3, D-91058 Erlangen, Peter.Wasserscheid@crt.cbi.uni-erlangen.de

Experimental Section

General Methods. N-(Trimethylsilyl) imidazole, Na[BF₄], and Na[ClO₄] were purchased from ACROS and were used without further purification. 1-Chlorododecane was purchased from Fluka and used as received. ¹H NMR and ¹³C NMR spectra were recorded on a JEOL 270 MHz NMR spectrometer operating at respective frequencies of 269.714 and 67.82 MHz with a probe temperature of 23 °C. Chemical shifts are reported relative to the peak for SiMe₄ using ¹H (residual) chemical shifts of the solvent as a secondary standard and are reported in ppm. Elemental analysis results were obtained from the Analytical Laboratories at the Friedrich-Alexander-University Erlangen-Nürnberg (Erlangen, Germany).

Preparation of [C₁₂C₁₂IM]Cl.¹ N-Trimethylsilylimidazole (4 mL, 28 mmol) was heated under reflux with 1-Chlorododecane (19.4 mL, 82 mmol) in toluene (30 mL) for 24 h under dry nitrogen. After complete removal of toluene, the product was re-crystallized from CH₂Cl₂/ether at 4 °C. White crystals of product were isolated by filtration, washed with diethyl ether, and dried in vacuo. Yield: 4.2 g (34 %). ¹H NMR (270 MHz, DMSO-d₆): δ 9.37 (s, 1H, imidazole C(2)H), 7.80 (d, *J* = 1.5 Hz, 2H, imidazole CH=CH), 4.12 (t, *J* = 6.8 Hz, 4H, NCH₂), 1.73 (quintet, *J* = 7.1 Hz, NCH₂CH₂), 1.17 (m, 36H, (CH₂)_n), 0.79 (t, *J* = 6.2 Hz, CH₃). ¹³C{¹H} NMR (67.5 MHz, DMSO-d₆): δ 214.96, 136.10, 122.49, 48.80, 31.32, 29.27, 29.05, 28.95, 28.90, 28.75, 28.36, 25.45, 22.12, 13.95. Anal. Calcd for C₂₇H₅₃N₂Cl: C, 73.51; H, 12.11; N, 6.35. Found: C, 73.41; H, 12.49; N, 6.36.

Preparation of 1 [C₁₂C₁₂IM][BF₄]. To a solution of 1,3-dodecylimidazolium chloride (1 g, 2.27 mmol) in acetone (10 mL) was added Na[BF₄] (0.299 g, 2.72 mmol). The mixture was stirred for 2 days, followed by removal of the solvent. CH₂Cl₂ (10 mL) was then added to the mixture followed by filtration. The solution was evaporated to dryness to give 1-dodecyl-3-methylimidazolium tetrafluoroborate. Yield: 1.05 g, (94 %). ¹H NMR (270 MHz, DMSO-d₆): δ 9.15 (s, 1H, imidazole C(2)H), 7.76 (s, 2H, imidazole CH=CH), 4.12 (t, *J* = 6.8 Hz, 4H, NCH₂), 1.74 (quintet, *J* = 7.1 Hz, NCH₂CH₂), 1.19 (m, 36H, (CH₂)_n), 0.81 (t, *J* = 6.5 Hz, CH₃). ¹³C{¹H} NMR (67.5 MHz, DMSO-d₆): δ 215.46, 136.46, 123.02, 49.37, 31.84, 29.74, 29.57, 29.47, 29.40, 29.27, 28.86, 25.97, 22.64, 14.45. Anal. Calcd for C₂₇H₅₃N₂BF₄: C, 65.84; H, 10.85; N, 5.69. Found: C, 65.91; H, 11.14; N, 5.81.

Preparation of 2 [C₁₂C₁₂IM][ClO₄]. Na[ClO₄] (0.4 g, 3.27 mmol) was added to a solution of 1,3-dodecylimidazolium chloride (1.2 g, 2.72 mmol) in 10 mL dichloromethane and stirred for 2 days. The suspension was filtered to remove the precipitated chloride salt and the organic phase was washed with small volumes of water (ca. 30 mL) until no precipitation of AgCl occurred in the aqueous phase on addition of a concentrated Ag[NO₃] solution. The organic phase was then washed with water to ensure complete removal of the chloride salt. The solvent was removed in vacuo and the resulting ionic liquid was dried at 100 °C in vacuo for 24 h. Yield: 1.25 g, (91 %). ¹H NMR (270 MHz, DMSO-*d*₆): δ 9.17 (s, 1H, imidazole C(2)H), 7.78 (d, *J* = 1.5 Hz, 2H, imidazole CH=CH), 4.14 (t, *J* = 7.0 Hz, 4H, NCH₂), 1.77 (quintet, *J* = 6.8 Hz, NCH₂CH₂), 1.22 (m, 36H, (CH₂)_n), 0.84 (t, *J* = 6.5 Hz, CH₃). ¹³C{¹H} NMR (67.5 MHz, DMSO-*d*₆): δ 215.46, 136.48, 123.02, 48.84, 31.31, 29.21, 29.04, 28.93, 28.87, 28.73, 28.32, 25.43, 22.12, 13.96. Anal. Calcd for C₂₇H₅₃N₂ClO₄: C, 64.19; H, 10.57; N, 5.55. Found: C, 64.65; H, 10.69; N, 5.60.

References

1. Harlow, K. J.; Hill, A. F.; Welton, T. *Synthesis*, **1996**, 697.

X-Ray Crystal Structure Determination Details:

CCDC-XXXXXX for **1**, [C₁₂C₁₂IM][BF₄], and CCDC-XXXXXX for **2**, [C₁₂C₁₂IM][ClO₄], contain the supplementary crystallographic data for this paper. These data can be obtained free of charge via http://www.ccdc.cam.ac.uk/data_request/cif (or from Cambridge Crystallographic Data Centre, 12 Union Road, Cambridge, CB2 1EZ, UK (fax: ++44-1223-336-033; e-mail: deposit@ccdc.cam.ac.uk)).

Colorless plates of both C₂₇H₅₃BF₄N₂ (**1**) and C₂₇H₅₃N₂ClO₄ (**2**) were grown by layering a CH₂Cl₂ solution of the corresponding imidazolium salt with diethyl ether. Suitable single crystals were embedded in protective perfluoropolyalkyether oil and transferred to the cold nitrogen gas stream of the diffractometer. Intensity data were collected at 200 K on a Bruker-Nonius KappaCCD diffractometer using graphite monochromatized MoK_α radiation (λ = 0.71073 Å). Data were corrected for Lorentz and polarization effects, semiempirical absorption corrections were performed on the basis of multiple scans using SADABS.^[1] The

structures were solved by direct methods and refined by full-matrix least-squares procedures on F^2 using *SHELXTL NT* 6.12.^[2]

$[\text{C}_{12}\text{C}_{12}\text{IM}][\text{BF}_4]$ (**1**) crystallizes with two independent cations and anions in the asymmetric unit. One of the imidazolium cations is disordered in one of the side arms. Two alternative positions were refined for the atoms C46, C48, C50, C53 resulting in a site occupancy of 78.7(8) % for the major fraction and 21.3(8) % for the minor part (C46A, C48A, C50A and C53A). Both $[\text{BF}_4]^-$ anions are subjected to rotational disorder around one of the B-F bonds. The two alternative positions refined yielded site occupancies of 61.0(11) and 39.0(11) % for F12 – F14 and F12A – F14A, respectively and 70.1(8) and 29.9(8) % for F22 – F24 and F22A – F24A, respectively. SIMU and SADI restraints were used in the refinement of the disorder. All non-hydrogen atoms were refined with anisotropic displacement parameters. All hydrogen atoms were placed in positions of optimized geometry, their isotropic displacement parameters were tied to those of the corresponding carrier atoms by a factor of either 1.2 or 1.5.

Table S1. Crystallographic data, data collection, and refinement details of

$[\text{C}_{12}\text{C}_{12}\text{IM}][\text{BF}_4]$ (**1**) and $[\text{C}_{12}\text{C}_{12}\text{IM}][\text{ClO}_4]$ (**2**)

	1	2
Empirical formula	$\text{C}_{27}\text{H}_{53}\text{BF}_4\text{N}_2$	$\text{C}_{27}\text{H}_{53}\text{ClN}_2\text{O}_4$
Mol. Weight	492.52	505.16
Crystal size	$0.28 \times 0.27 \times 0.06$	$0.44 \times 0.30 \times 0.12$
Temperature [K]	200	200
Crystal system	triclinic	monoclinic
Space group	$P\bar{1}$ (no. 2)	$P2_1/n$ (no. 14)
a [\AA]	8.5500(7)	7.6633(6)
b [\AA]	8.7636(6)	10.1450(5)
c [\AA]	41.352(3)	38.800(3)
α [$^\circ$]	90.194(7)	90
β [$^\circ$]	92.173(7)	90.678(7)
γ [$^\circ$]	100.503(7)	90
V [\AA^3]	3044.2(4)	3016.3(4)
Z	4	4
ρ [g/cm^3] (calc.)	1.075	1.112

μ [mm ⁻¹]	0.078	0.158
$F(000)$	1080	1112
$T_{\min}; T_{\max}$	0.971; 0.994	0.875; 0.981
2 θ interval [°]	$6.3 \leq 2\theta \leq 50.8$	$6.6 \leq 2\theta \leq 51.4$
Collected reflections	66463	45939
Independent reflections;	11142;	5730;
R_{int}	0.1711	0.0436
Observed reflections	4770	4373
$[I \geq 2\sigma(I)]$		
No. refined parameters	709	309
wR_2 (all data)	0.1883	0.1266
$R_1(F_0 \geq 4\sigma(F))$	0.0628	0.0507
GooF on F^2	0.930	1.043
$\Delta\rho_{\max/\min}$	0.240 / -0.211	0.360 / -0.288

References:

- [¹] *SADABS 2.06*, Bruker AXS, Inc., **2002**, Madison WI., U.S.A.
[²] *SHELXTL NT 6.12*, Bruker AXS, Inc., **2002**, Madison WI., U.S.A.

Graphical Representations

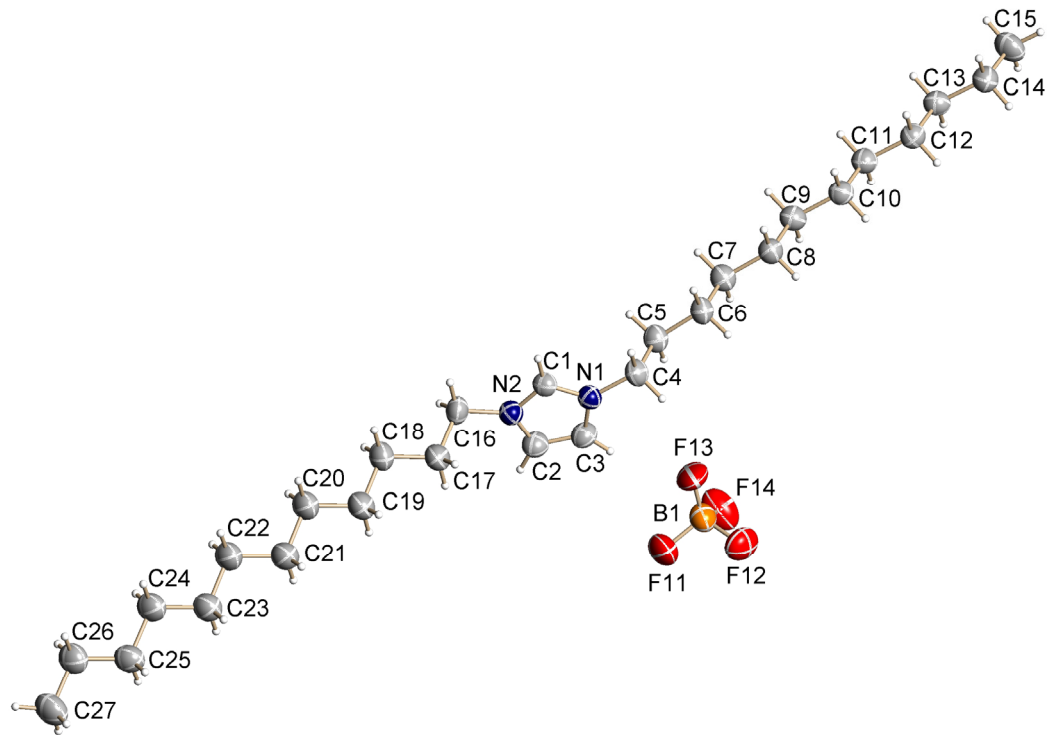


Figure S1a:

Thermal ellipsoid plot of [C₁₂C₁₂IM][BF₄] (**1**) with labeling scheme of the non-hydrogen atoms (50 % probability ellipsoids, H atoms drawn as spheres of arbitrary size, disordered part of the BF₄ omitted for clarity), molecule A of two independent molecules.

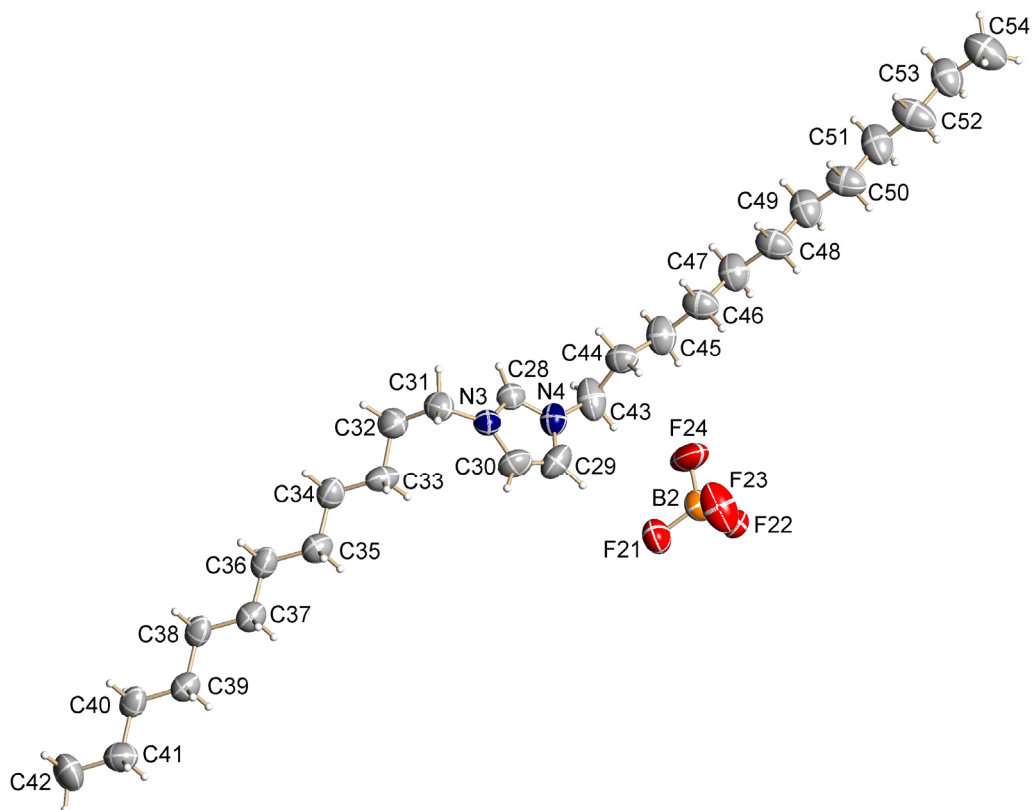


Figure S1b:

Thermal ellipsoid plot of [C₁₂C₁₂IM][BF₄] (**1**) with labeling scheme of the non-hydrogen atoms (50 % probability ellipsoids, H atoms drawn as spheres of arbitrary size, disordered parts of the cation and the BF₄ omitted for clarity), molecule B of two independent molecules.

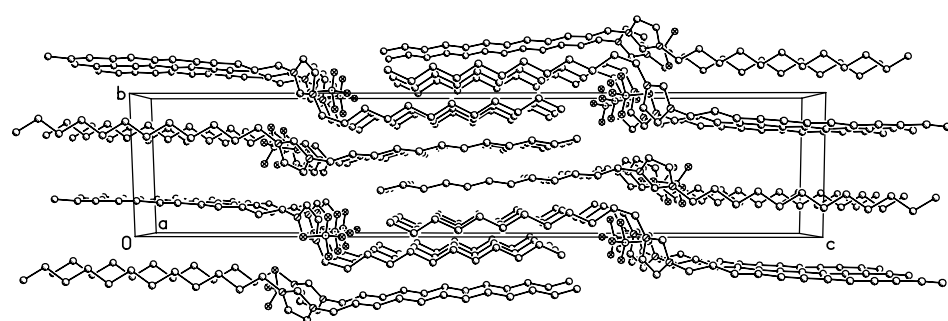


Figure S1c:

Packing diagram of [C₁₂C₁₂IM][BF₄] (**1**), view along the crystallographic *a* axis.

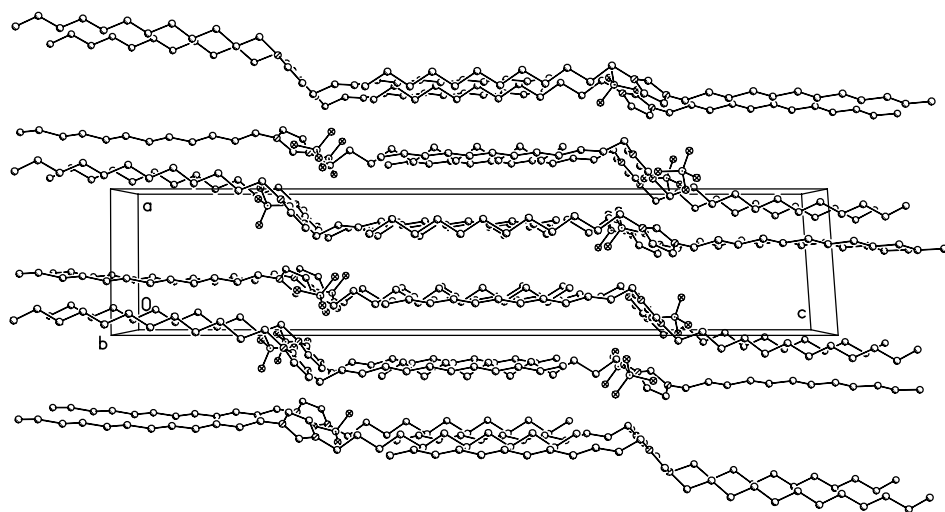


Figure S1d:

Packing diagram of $[C_{12}C_{12}IM][BF_4]$ (**1**), view along the crystallographic *b* axis.

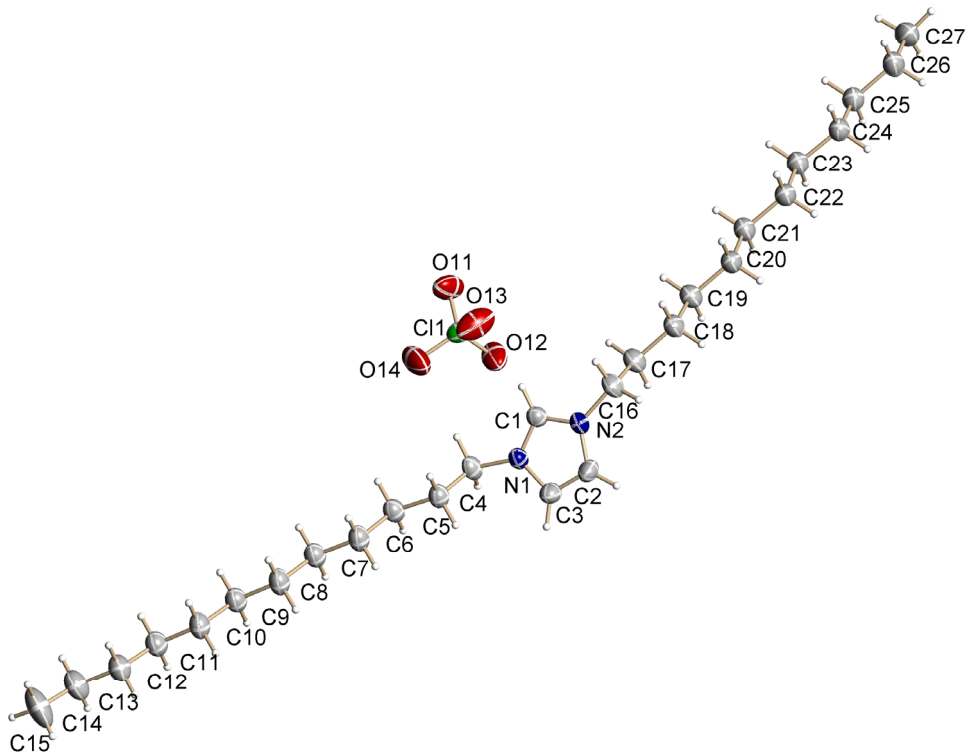


Figure S2a:

Thermal ellipsoid plot of $[C_{12}C_{12}IM][ClO_4]$ (**2**) with labeling scheme of the non-hydrogen atoms (50 % probability ellipsoids, H atoms drawn as spheres of arbitrary size).

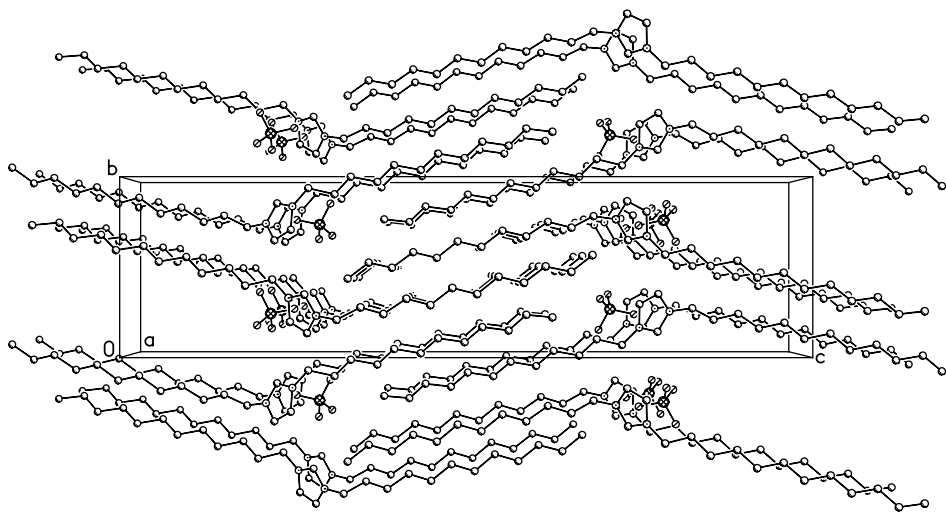


Figure S2b:

Packing diagram of $[C_{12}C_{12}IM][ClO_4]$ (2), view along the crystallographic a axis.

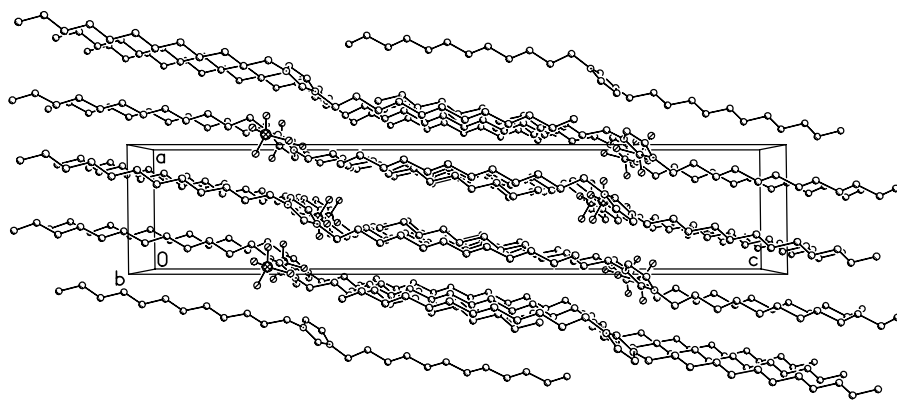


Figure S2c:

Packing diagram of $[C_{12}C_{12}IM][ClO_4]$ (2), view along the crystallographic b axis.

Characterization and Physico-Chemical Properties:

Thermal measurements. Differential scanning calorimetry (DSC) was performed with a computer-controlled Phoenix DSC 204 F1 thermal analyser (Netzsch, Selb, D) with argon as protection gas. The samples were placed under inert conditions in aluminium pans, which were cold-sealed. Measurements were carried out with a thermal ramp of 5 K/min. Experimental data are displayed in such a way that exothermic peaks occur at negative heat flow and endothermic peaks at positive heat flow. Given temperatures correspond to the onset of the respective thermal process.

Polarizing Optical Microscopy. Optical analyses were carried out by hot-stage polarized optical microscopy (POM) with an Axio Imager A1 microscope (Carl Zeiss MicroImaging GmbH, Göttingen, D) equipped with a hot stage, THMS600 (Linkam Scientific Instruments Ltd, Surrey, UK), and temperature controller, Linkam TMS 94 (Linkam Scientific Instruments Ltd, Surrey, UK). The images were recorded as movies with a digital camera after initial heating during then cooling stage. For the measurement the sample was placed under inert atmosphere between two hermetically sealed cover slips.

Differential Scanning Calorimetry (DSC) Data

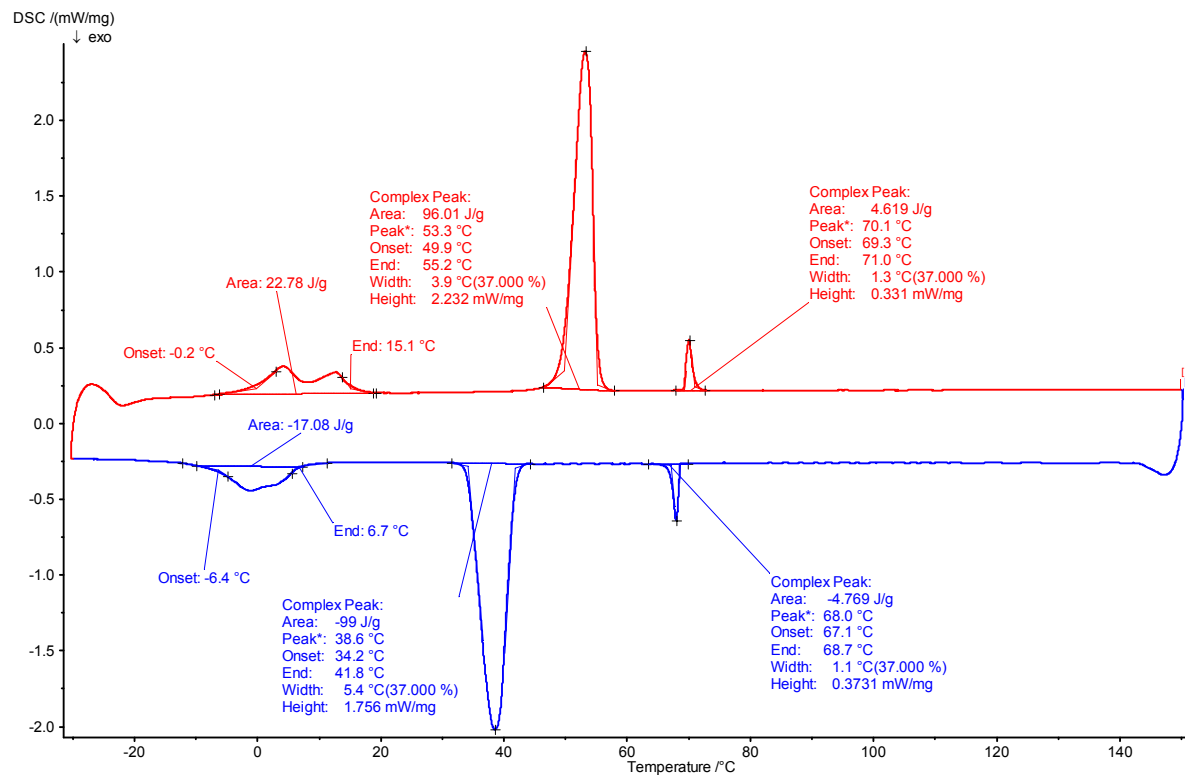


Figure S3: DSC of $[C_{12}C_{12}Im][BF_4]$ **1**

1st cooling cycle in blue (bottom), 2nd heating cycle in red (top).

(Thermal effects below 30 °C are attributed to solid-solid phase transitions.)

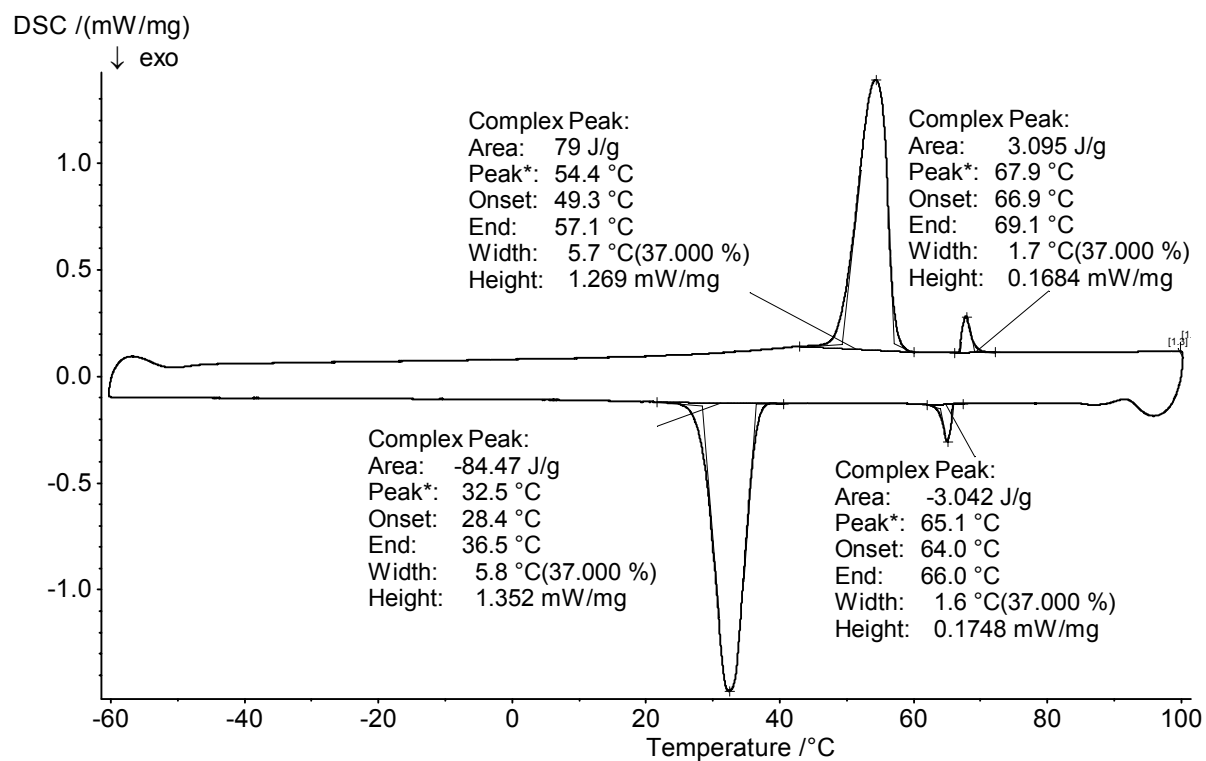
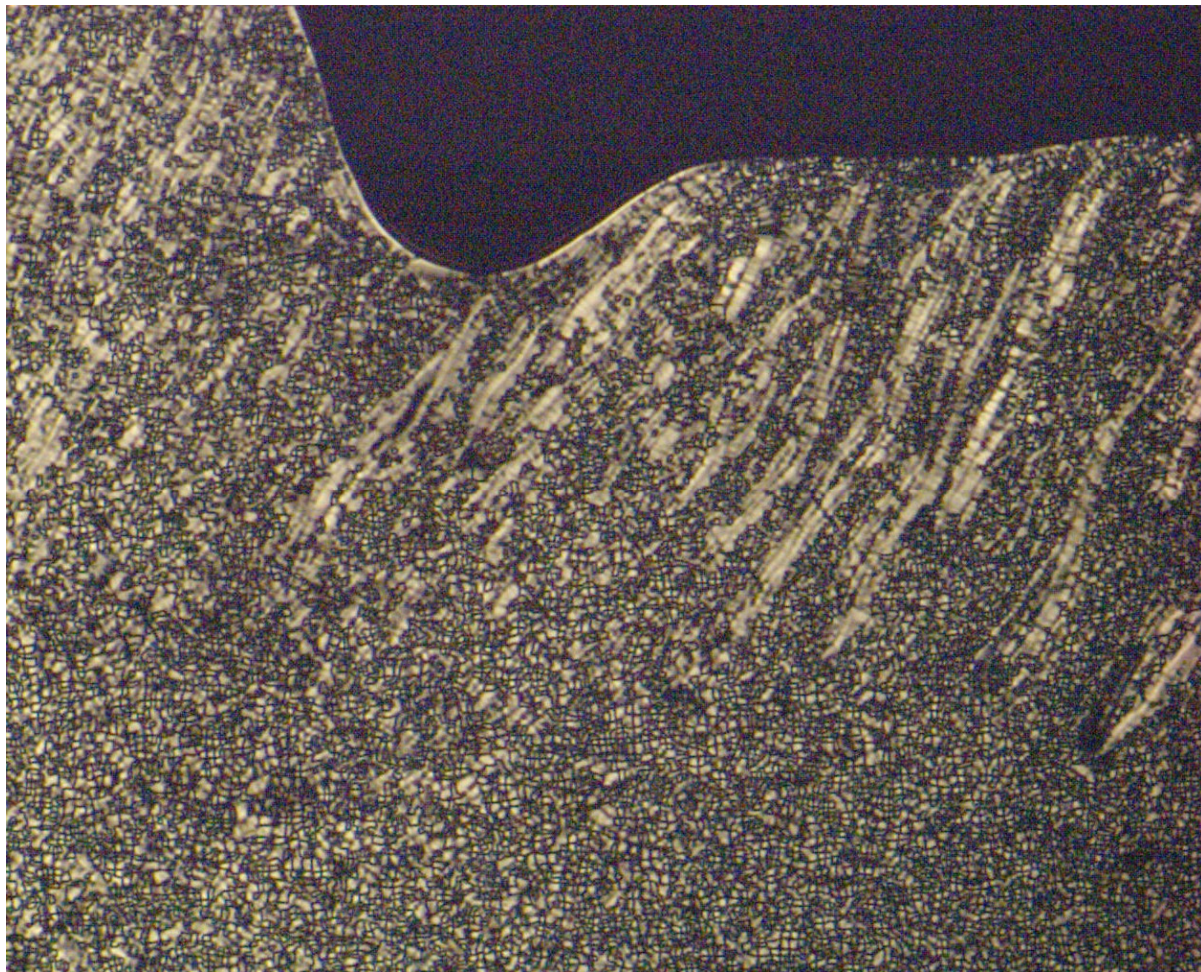
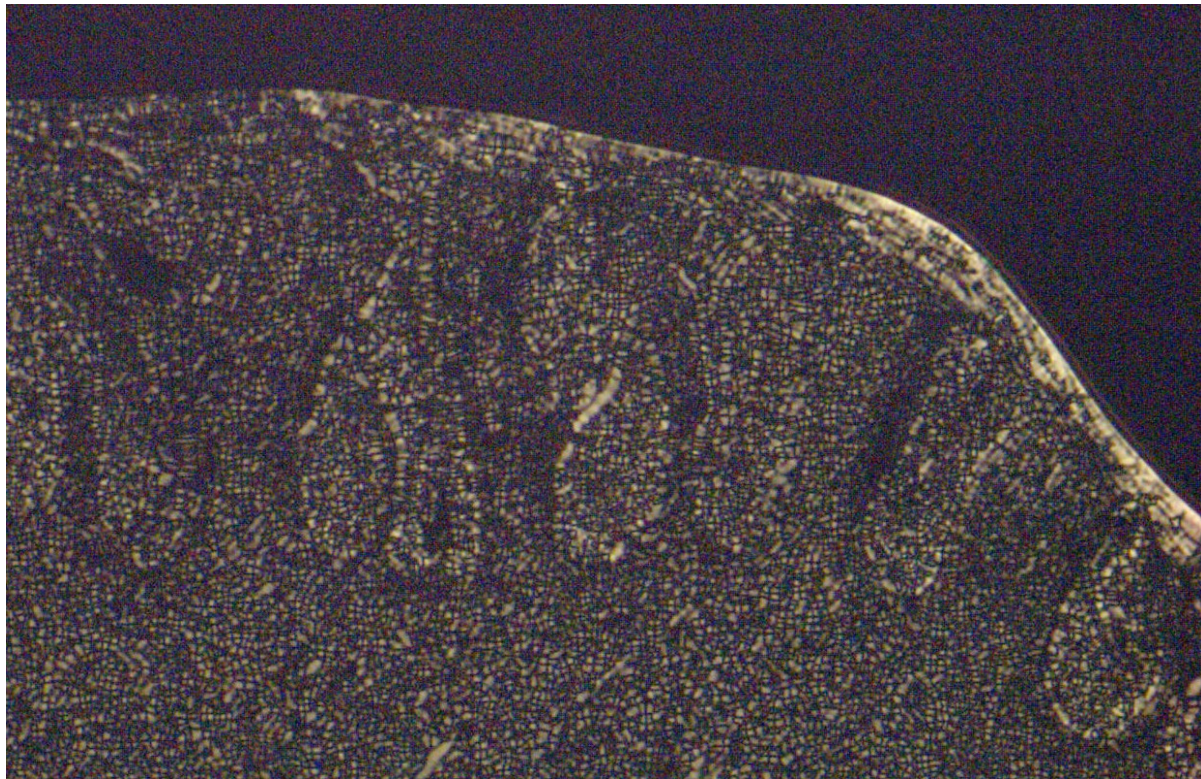


Figure S4: DSC of $[\text{C}_{12}\text{C}_{12}\text{IM}][\text{ClO}_4]$ **2**
1st cooling cycle (bottom), 2nd heating cycle (top).

Polarized Optical Microscopy data



S5 a: Polarized light optical microscope picture of $[C_{12}C_{12}IM][BF_4]$ (**1**) at $T = 50\text{ }^{\circ}\text{C}$.



S5b: Polarized light optical microscope picture of $[C_{12}C_{12}IM][ClO_4]$ **2** at $T = 42\text{ }^{\circ}\text{C}$